

## Supporting Information

### Iron Impregnated Cellulosic Carbon as an Effective Electrocatalyst for Seawater Oxidation

Sakila Khatun,<sup>a,b</sup> Chandni Das<sup>a,b</sup> and Poulomi Roy \*<sup>a,b</sup>

<sup>a</sup>CSIR– Central Mechanical Engineering Research Institute (CMERI), Mahatma Gandhi Avenue, Durgapur 713209, West Bengal, India.

<sup>b</sup>Academy of Scientific and Innovative Research (AcSIR), Ghaziabad, Uttar Pradesh 201002, India.

E-mail: poulomiroy@yahoo.com

#### Figures.

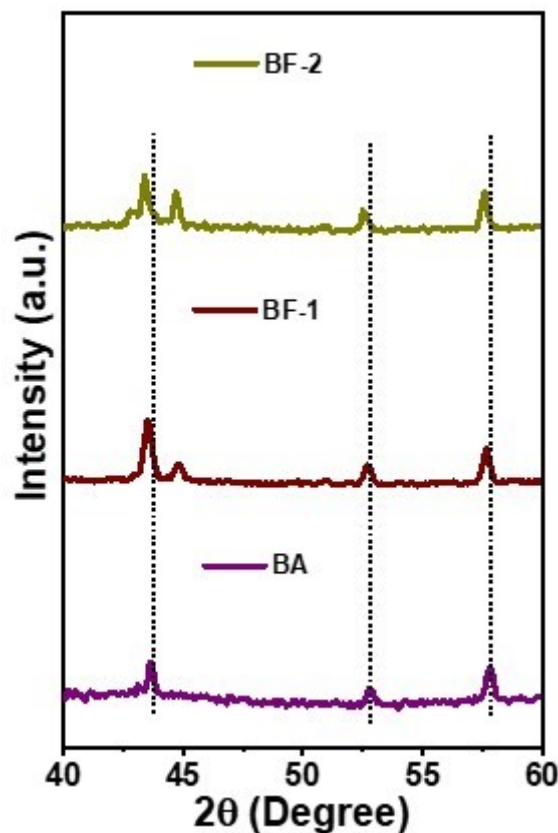


**Fig S1.** Magnified view of XRD pattern of all developed BA and BF samples.

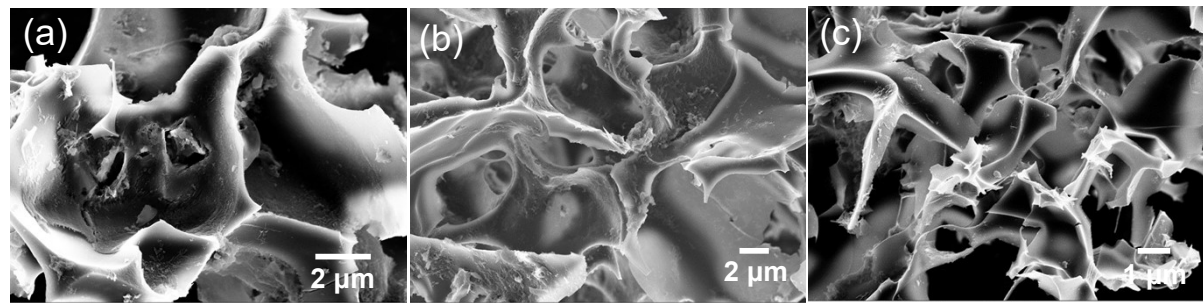


**Fig S2.** FESEM image of (a) BA, (b) BF-1 and (c) BF-2 samples.

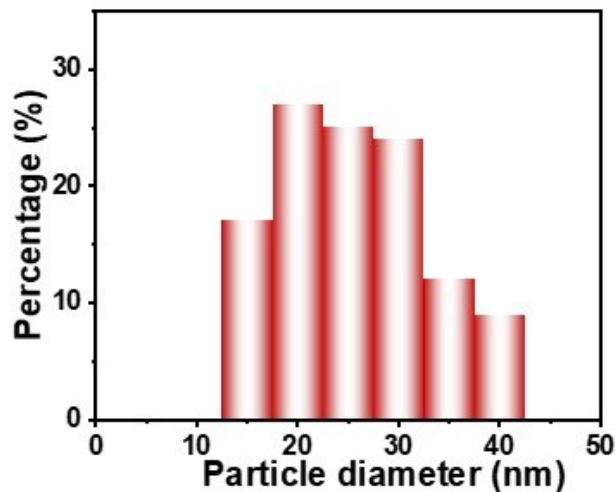


**Fig S3.** Statistical particle size distribution of Fe nanoparticle for BF-1 sample.

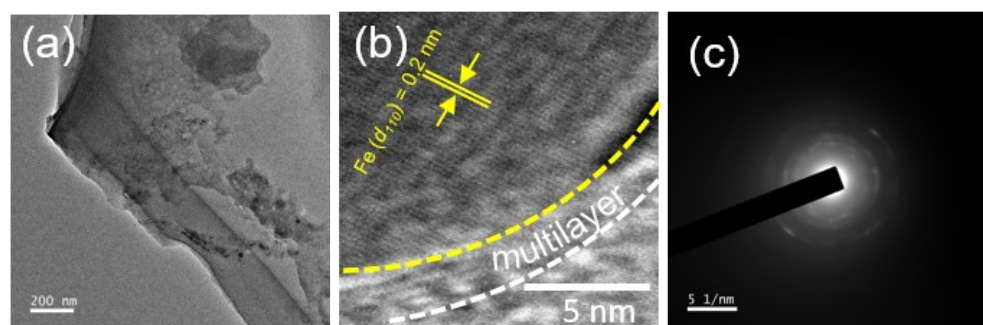


**Fig S4.** (a) TEM, (b) HRTEM and (c) corresponding SAED pattern of BF-2 sample.

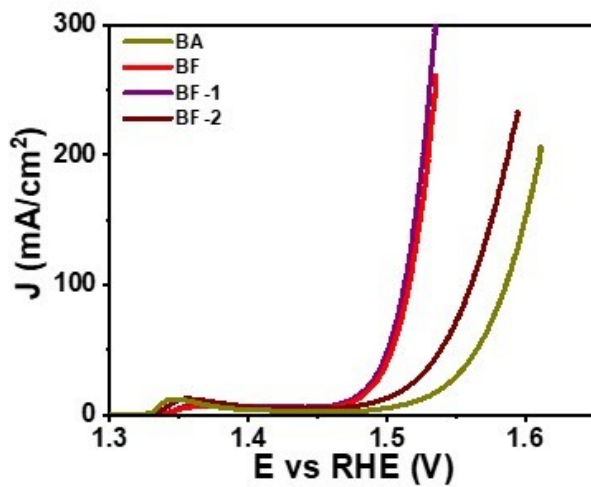


**Fig S5.** LSV plot of all developed samples in 1 M KOH electrolyte solution.

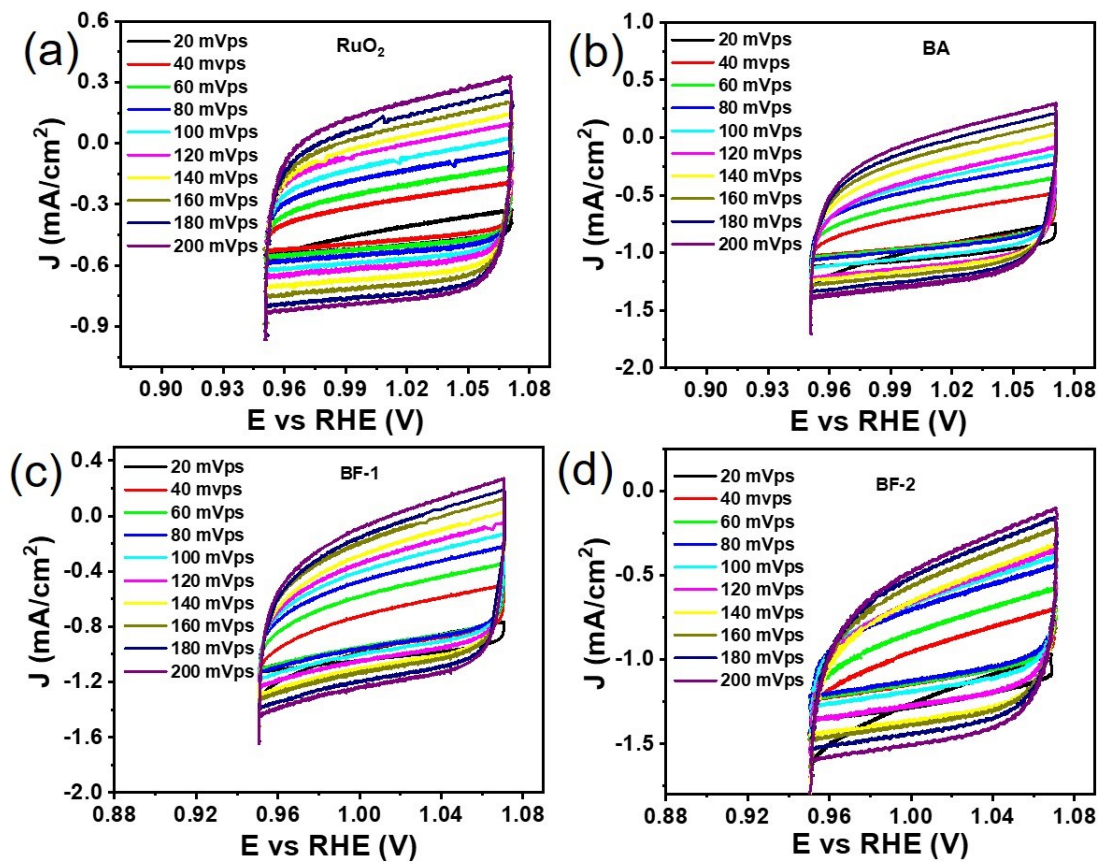


**Fig S6.** (a-d) Cyclic voltammograms (CV) plots recorded at various scan rate in non-faradaic region for (a) conventional  $\text{RuO}_2$ , (b) BA, (c) BF-1 and (d) BF-2 samples towards OER process in alkaline media.

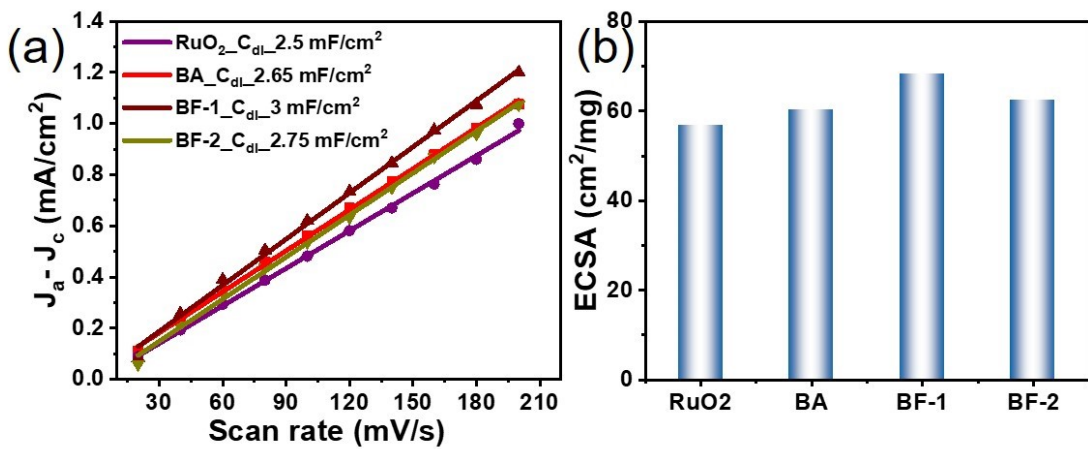


**Fig S7.** (a) Current density plot against scan rate to determine double layer capacitance ( $C_{dl}$ ) value and (b) bar diagram representing ECSA determined for samples towards OER process in alkaline media.

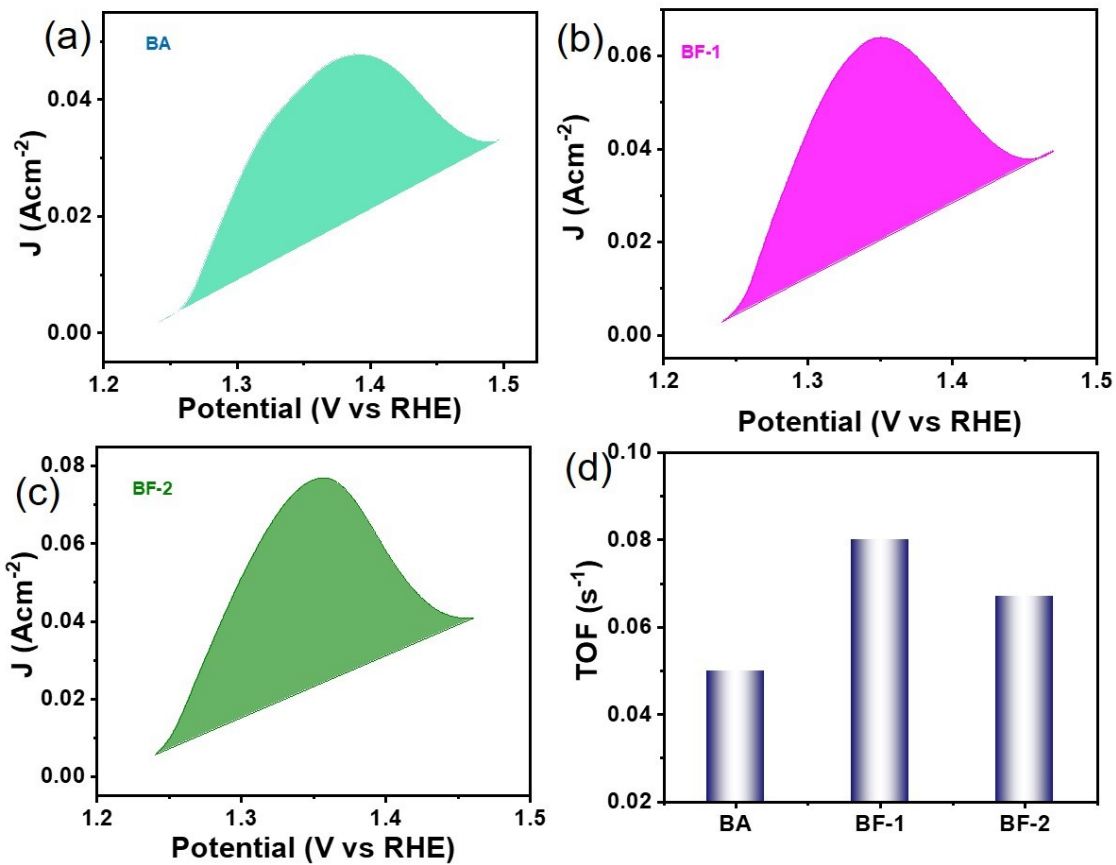


**Fig S8.** (a-c) Oxidation peak area of CV curves at 20 mV s<sup>-1</sup> scan rate for (a) BA, (b) BF-1 and (c) BF-2 samples for OER process. (d) Bar diagram of turn over frequency (TOF) value of all developed samples for OER process at 320 mV overpotential.

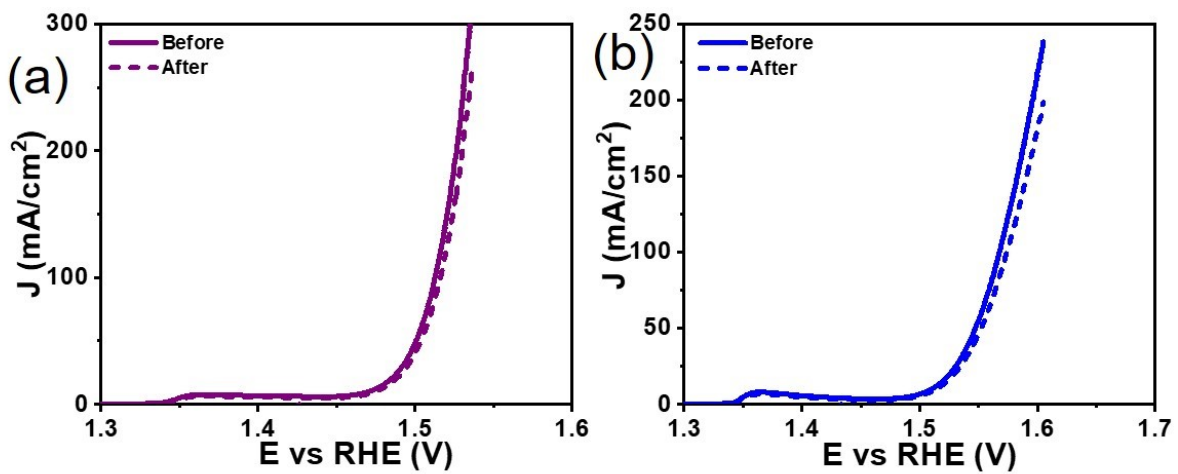


**Fig S9.** LSV plots of optimum BF-1 electrocatalyst before and after chronoamperometry operation towards electrochemical OER performance in (a) 1 M KOH and (b) 1 M KOH + seawater electrolytes.

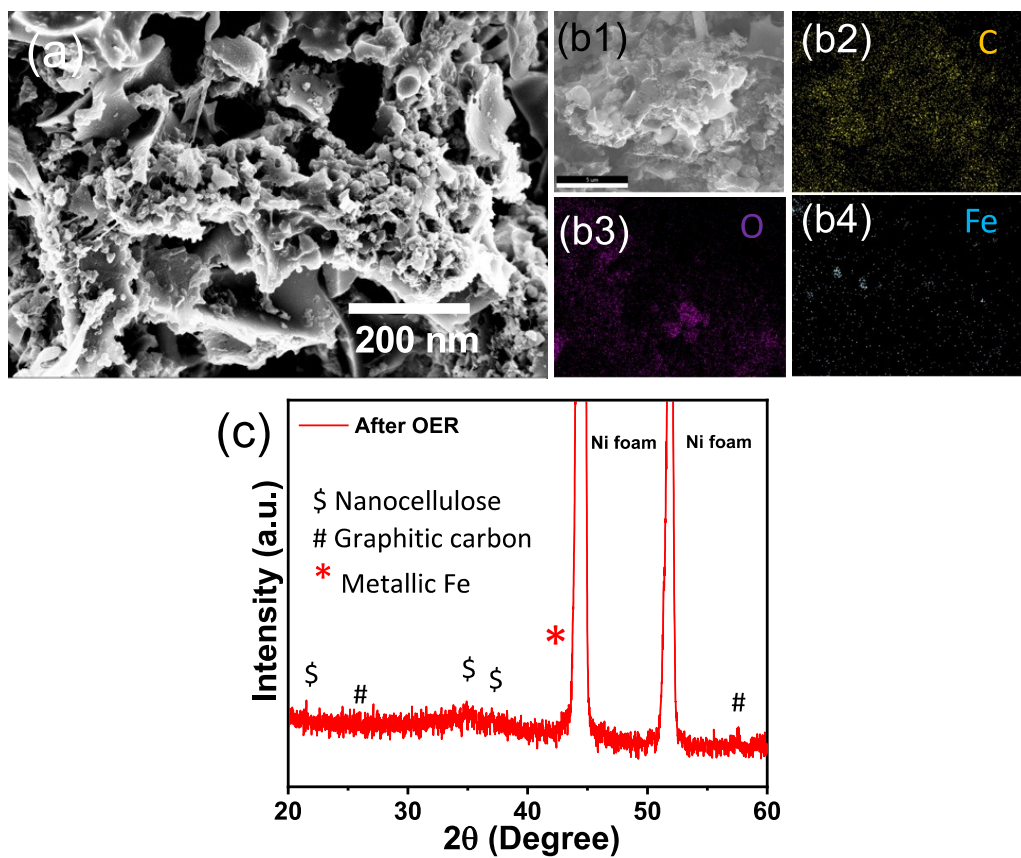


**Fig S10.** (a) FESEM image and (b1-b4) corresponding elemental mapping of BF-1 after stability test in alkaline seawater electrolyte. (c) XRD pattern of BF-1 after stability test in alkaline seawater electrolyte.

**Tables.**

**Table S1.** EDX analysis showing weight% of the elements present in the resulting developed BA and BF-1 samples.

Sample	C	O	Fe
BA	86	14	0.0
BF	81	17	2
BF-1	78	16	6
BF-2	66	21	13

**Table S2.** Comparative table for the electrochemical parameters of all developed catalysts towards OER operation in 1 M KOH electrolyte solution.

Sample	$\eta_{10}$ (mV)	$\eta_{100}$ (mV)	Tafel slope (mV dec <sup>-1</sup> )	$R_{ct}$ ( $\Omega$ )	ECSA (cm <sup>2</sup> mg <sup>-1</sup> )
Ni foam	345	455	103	7.9	.....
RuO <sub>2</sub>	305	390	90	2.9	56
BA	288	355	68	1.12	60
BF-1	238	280	40	0.89	68.2
BF-2	260	329	54	1.11	62.5

**Table S3.** Comparative table for the electrochemical parameters of optimized BF-1 catalyst towards OER operation in different electrolyte solution.

Sample	$\eta_{10}$ (mV)	$\eta_{50}$ (mV)	$\eta_{100}$ (mV)	Tafel slope (mV dec <sup>-1</sup> )	$R_{ct}$ ( $\Omega$ )
<b>1 M KOH</b>	1.468	1.50	1.51	40	0.89
<b>1 M KOH + 1 M NaCl</b>	1.502	1.539	1.56	58	1.88
<b>1 M KOH + Seawater</b>	1.510	1.546	1.566	57	4.86

**Table S4.** Comparison table of electrocatalytic OER performance of various Fe as well as carbon based electrocatalyst in different electrolyte solution.

Catalysts	Electrolyte	Overpotential (mV)	Durability (h)	Ref.
Fe impregnated cellulosic carbon	1 M KOH	238 mV @ 10 mA cm <sup>-2</sup>	50	This work
	1 M KOH + Seawater	280 mV @ 10 mA cm <sup>-2</sup>	30	
Cellulosic Carbon	1 M KOH	288 mV @ 10 mA cm <sup>-2</sup>	...	
N-doped porous carbon	1 M KOH	314 mV @ 10 mA cm <sup>-2</sup>	8	1
Fe-N-C/FeP <sub>x</sub> /NPSC	1 M KOH	370 mV@ 10 mA cm <sup>-2</sup>	10	2
N, P doped carbon nanofiber encapsulated Fe <sub>3</sub> O <sub>4</sub> and FeP nanoparticles	1 M KOH	330 mV@ 10 mA cm <sup>-2</sup>	....	3
N, P dual doped graphene/carbon nanosheets (N, P-GCNS)	1 M KOH	340 mV@ 10 mA cm <sup>-2</sup>	4.5	4
N <sub>1</sub> -CoP@NPCNFs-900s	1 M KOH	266 mV@ 10 mA cm <sup>-2</sup>	.....	5
CQDs/NiFe-LDH	1 M KOH	235 mV @ 10 mA cm <sup>-2</sup>	.....	6

Ni <sub>0.9</sub> Fe <sub>0.1</sub> /Nanocarbon hybrid	1 M KOH	330 mV@ 10 mA cm <sup>-2</sup>	24	<a href="#">7</a>
N-Fe-Cu co-doped carbon	1 M KOH	362 mV@ 10 mA cm <sup>-2</sup>	20	<a href="#">8</a>
Fe-Co <sub>3</sub> O <sub>4</sub> /CNTs	1 M KOH	300 mV@ 10 mA cm <sup>-2</sup>	25	<a href="#">9</a>
Fe <sub>0.5</sub> Co <sub>0.5</sub> @NC/NCNS-800	1 M KOH	270 mV@ 10 mA cm <sup>-2</sup>	8	<a href="#">10</a>
(Ni <sub>x</sub> Fe <sub>1-x</sub> ) <sub>2</sub> P@graphitized carbon	1 M KOH	206 mV @ 10 mAcm <sup>-2</sup>	30	<a href="#">11</a>
Cr doped FeNi <sub>3</sub> /NiFe <sub>2</sub> O <sub>4</sub>	1 M KOH	246 mV @ 20 mAcm <sup>-2</sup>	200	<a href="#">12</a>
MnFeCr LTH	1 M KOH + Seawater	341 mV @ 100 mAcm <sup>-2</sup>	50	<a href="#">13</a>
Fe <sub>0.05</sub> CoNi LDH/NF	1 M KOH + Seawater	287 mV @ 10 mAcm <sup>-2</sup>	14	<a href="#">14</a>
Fe-NiMoSe@C	1 M KOH + Seawater	354 mV @ 500 mAcm <sup>-2</sup>	100	<a href="#">15</a>
Cr-CoFe LDH/NF	1 M KOH + Seawater	334 mV @ 500 mAcm <sup>-2</sup>	100	<a href="#">16</a>
S(-NiFe)OOH	1 M KOH + Seawater	300 mV @ 100 mAcm <sup>-2</sup>	100	<a href="#">17</a>
NiFeCrVMn HEA embedded LDH	1 M KOH + Seawater	300 mV @ 100 mAcm <sup>-2</sup>	110	<a href="#">18</a>
FeCoNiMnMo HEA	1 M KOH + Seawater	360 mV @ 100 mAcm <sup>-2</sup>	119	<a href="#">19</a>
NiCrCoFeMo layered hydroxide	1 M KOH + Seawater	258 mV @ 100 mAcm <sup>-2</sup>	50	<a href="#">20</a>

## References

- 1 C. Sathiskumar, S. Ramakrishnan, M. Vinothkannan, A. R. Kim, S. Karthikeyan and D. J. Yoo, *Nanomaterials*, 2020, **10**, 76.
- 2 P. Li, H. Wang, W. Fan, M. Huang, J. Shi, Z. Shi and S. Liu, *Chem. Eng. J.*, 2021, **421**, 129704.
- 3 M. Wang, C. Zhang, T. Meng, Z. Pu, H. Jin, D. He, J. Zhang and S. Mu, *J. Power Sources*, 2019, **413**, 367–375.
- 4 R. Li, Z. Wei and X. Gou, *ACS Catal.*, 2015, **5**, 4133–4142.
- 5 Z. Cui, J. Lin, J. Wu, J. Yu, J. Si and Q. Wang, *J. Alloys Compd.*, 2021, **854**, 156830.
- 6 D. Tang, J. Liu, X. Wu, R. Liu, X. Han, Y. Han, H. Huang, Y. Liu and Z. Kang, *ACS Appl. Mater. Interfaces*, 2014, **6**, 7918-7925.
- 7 X. Zhang, H. Xu, X. Li, Y. Li, T. Yang and Y. Liang, *ACS Catal.*, 2016, **6**, 580-588.
- 8 Q. He, H. Liu, P. Tan, J. Xie, S. Si and J. Pan, *J. Solid State Chem.*, 2021, **299**, 122179.
- 9 H. Begum and S. Jeon, *Int. J. Hydrogen Energy*, 2018, **43**, 5522-5529.
- 10 M. Li, T. Liu, X. Bo, M. Zhou and L. Guo, *J. Mater. Chem. A*, 2017, **5**, 5413.
- 11 H. Zhao, Y. Wang, L. Fang, W. Fu, X. Yang, S. You, P. Luo, H. Zhang and Y. Wang, *J. Mater. Chem. A*, 2019, **7**, 20357.
- 12 S. Khatun, S. Pal and P. Roy, *J. Alloys Compd.*, 2024, **977**, 173393.
- 13 S. Pal, K. Shimizu, S. Khatun, S. Singha, S. Watanabe and P. Roy, *J. Mater. Chem. A*, 2023, **11**, 12151.
- 14 A. Gupta, H. K. Sadhanala, A. Gedanken, *Electrochim. acta* 2023, **470**, 143269.
- 15 X. Xu, S. Zhang, Q. Zhang, S. Chen, Y. Wu, Z. Sun, *ACS Sustainable Chem. Eng.* 2023, **11**, 15338-15349.
- 16 Y. Yao, C. Yang, S. Sun, H. Zhang, M. Geng, X. He, K. Dong, Y. Luo, D. Zheng, W. Zhunag, S. Alfaifi, A. Farouk, M. S. Hamdy, B. Tang, S. Zhu, X. Sun, W. Hu, *Small* 2024, **20**, 2307294.
- 17 L. Yu, L. Wu, B. McElhenny, S. Song, D. Luo, F. Zhang, Y. Yu, S. Chen, Z. Ren, *Energy Environ. Sci.* 2020, **13**, 3439-3446.
- 18 S. Khatun, K. Shimizu, S. Pal, S. Nandi, S. Watanabe and P. Roy, *Small*, 2024, 2402720.
- 19 P. Li, Y. Yao, W. Ouyang, Z. Liu, H. Yin, D. Wang, *J. Mater. Sci. Technol.* 2023, **138**, 29–35.
- 20 S. Pal, S. Khatun, P. Roy, *Mater. Adv.* 2024, **5**, 5156-5166.